Available online at www.sciencedirect.com
SCIENCE DIRECT®
Journal of Nuclear Materials 355 (2006) 54–67
journal of nuclear materials
www.elsevier.com/locate/jnucmat

Water diffusion in the simulated French nuclear waste glass SON 68 contacting silica rich solutions: Experimental and modeling

K. Ferrand *, A. Abdelouas, B. Grambow

SUBATECH – EMN-CNRS/IN2P3-Université de Nantes, 4 rue Alfred Kastler – La Chantrerie, B.P. 20722, 44307 Nantes cedex 03, France

Received 6 June 2005; accepted 20 April 2006

Abstract

To understand the role of water diffusion on the long-term nuclear waste glass alteration, dynamic experiments were conducted with the borosilicate SON 68 glass in synthetic solutions enriched in Si, Na and B at 50 and 90 °C. The water entering the glass exists to 80% in the form of molecular H_2O and to 20% in the form of SiOH. The ratio of H/Na was 2.6 ± 0.3, indicating a complex mechanism including water diffusion and ionic-exchange. It was in agreement with model calculations based on glass structural units such as reedmergnerite and B_2O_3. Water diffusion coefficients in the glass, determined by modeling of the experimental data, were between 2×10^{-21} and 6×10^{-23} $m^2\,s^{-1}$. Finally, under HLW disposal conditions, where interaction of nuclear glass with groundwater is expected to maintain saturation conditions, it is likely that water diffusion will contribute to the control of the glass alteration and the release of radionuclides.

1. Introduction

In France, fission products resulting from spent nuclear fuel reprocessing are being vitrified in La Hague facility. The resulting highly radioactive glass is stored at the surface waiting for deep geological disposal. A multi-barrier confinement system shall limit both water access to the glass and release of the radioactivity, but the alteration of the glass in contact with groundwater cannot be excluded for long-term. In contact with glass, water diffuses into the glass network and ion exchange occurs between protons and network-modifying alkali metal ions [1–6]. This results in the formation of a de-alkalized hydrated glass surface. In the following reaction step, the hydrated silicate network becomes hydrolyzed and certain network forming glass constituents dissolve leaving behind a gel-like surface layer often covered with or reacted into secondary phases (clays, zeolites) [7–9]. Glass constituents such as boron and lithium, which are not incorporated into this surface layer, are released congruently into the aqueous phase. Boron and lithium are often used as dissolution tracers in corrosion experiments [10–13]. During this reaction step, water diffusion and ion exchange continue at the reaction front

* Corresponding author. Tel.: +003214333128.
E-mail address: karine.ferrand@sckcen.be (K. Ferrand).

0022-3115/$ - see front matter © 2006 Elsevier B.V. All rights reserved.
doi:10.1016/j.jnucmat.2006.04.005

between the pristine glass and the gel layer, but this process is not rate limiting because the hydrated alkali-depleted surface becomes dissolved under steady state conditions with the same rate by which it is formed. In static leaching tests, dissolved glass constituents, mainly silica, accumulate in solution and lead to a decrease of corrosion rates with time, indicating either affinity controlled glass corrosion and /or solution stabilized protective layer formation [10–18]. For static conditions, Grambow and Müller [19] proposed that water diffusion may become rate limiting. This process may have to be taken into account in the modeling of long-term glass dissolution, when the affinity for dissolution of the alkali depleted surface tends to zero. Other authors have also shown the importance of ionic exchange [20–22].

The objective of the present work is to study the role of water diffusion in the long-term alteration of the French borosilicate nuclear waste glass SON 68 in dynamic experiments and in solutions saturated or supersaturated in dissolved silicon, and rich in B and Na, preventing the formation of secondary phases. Under these conditions neither the affinity rate law nor Si transport processes through a potentially protective gel layer are rate limiting. Such Si saturated conditions are expected in the limited void spaces of glass canisters in geological disposal locations. Experimental tests and modeling were conducted to determine the water diffusion coefficients in the glass.

Table 1
Composition of the simulated French nuclear waste SON 68 in wt%

Oxide		Wt%
A	SiO_2	45.48
B	Al_2O_3	4.91
C	B_2O_3	14.02
D	Na_2O	9.86
E	CaO	4.04
F	Fe_2O_3	2.91
G	NiO	0.74
H	Cr_2O_3	0.51
I	P_2O_5	0.28
J	ZrO_2	2.65
K	Li_2O	1.98
L	ZnO	2.50
M	SrO	0.33
N	Y_2O_3	0.20
O	MoO_3	1.70
P	MnO_2	0.72
Q	CoO	0.12
R	Ag_2O	0.03
S	CdO	0.03
T	SnO_2	0.02
U	SbO_2	0.01
V	TeO_2	0.23
W	Cs_2O	1.42
X	BaO	0.60
Y	La_2O_3	0.90
Z	Ce_2O_3	0.93
AA	Pr_2O_3	0.44
AB	Nd_2O_3	1.59
AC	UO_2	0.52
AD	ThO_2	0.33

2. Experimental

2.1. Materials and procedure

Alteration experiments at 50 and 90 °C were conducted with the simulated French nuclear waste SON 68 glass in a solution rich in Si, B and Na. The glass composition is given in Table 1. Two types of powdered glass were used as samples: one with an average particle diameter in the order of 20 μm and a BET (Kr) specific surface area of 0.51 $m^2\,g^{-1}$ (glass samples denoted d20) and the other with an average particle diameter in the order of 5 μm and a BET (Kr) specific surface area of 1.39 $m^2\,g^{-1}$ (glass samples denoted d5). Chips, with an average thickness of 100 μm and a geometric surface area of about 9 cm^2 were also used.

To simulate conditions of solution saturation of dissolved glass constituents with respect to the dissolving glass surface, a leachant solution was prepared enriched in silicon, boron and sodium. As reference chemical composition for this solution we used experimental data for SON 68 glass alteration for 189 days in an air saturated static system at 90 °C in de-ionized water with a geometric S/V ratio of $2\times10^4\,m^{-1}$ [23]. The reported final pH was about 9.52 at the end of the experiment. The synthetic solution was prepared by dissolving high purity chemicals, including SiO_2–NaOH and $Na_2B_4O_7$ in de-ionized water at 25 °C. The experimentally measured concentrations of Mo, Li and Cs were not simulated in the synthetic leachant solution in order to increase the sensitivity for these elements in the leaching experiments. The final silicon, boron and sodium concentrations were in the order of 120, 380 and 1015 ppm, respectively, and the pH (25 °C) was near 12. In some experiments the silicon concentration was set as 240 ppm to increase the degree of supersaturation. The pH (25 °C) was decreased from 12 to 9.8, by equilibration

with the atmosphere, the equilibration time was shortened by bubbling with Ar/CO_2 (90/10). To study the effect of pH on water diffusion in the glass, the pH (25 °C) of synthetic solution was further decreased in some experiments from about 9.8 to either 4.8 or 7.2 by addition of high purity HNO_3 (60%), and of acetic acid/sodium acetate or citric acid/caustic soda, as chemical buffers respectively.

Most of the experiments were conducted under dynamic leach conditions in order to keep solution composition constant and to minimize the formation of secondary phases and the accumulation of dissolved glass constituents. Formation of secondary phases is known to enhance the alteration rate of glasses [24–26] under certain conditions. This may interfere with the role of water diffusion on glass alteration. In the dynamic experiments, a peristaltic pump injected the leachant solution through a Teflon® reactor of a total volume of 35 mL containing the powdered glass samples or the chip. Experiments were conducted at 50 or 90 °C. The leachant flow rate was fixed at 0.6 mL h^{-1}. The outlet solution was collected in a bottle and an aliquot was diluted with HNO_3 2% UP and stored at 4 °C prior to chemical analyses. During experiments, the pH was monitored at room temperature.

In addition, few static experiments were conducted according to MCC-1 standard procedure to test whether the first order rate law holds in our tests, to identify the forward reaction rate constant and to determine the saturation concentration of dissolved silica with respect to the hydrated glass surface. The determination of this saturation concentration should confirm that the synthetic solution used in the dynamic tests (120 and 240 ppm Si) represents the saturation conditions well. In these experiments, the leachant was composed only of solutions of NaOH and $Na_2B_4O_7$ in carbonate saturated water and silicon concentration was varied from 0 to 240 ppm. Experiments were conducted in Teflon® reactors at 90 °C with 50 mg of glass powder (sample d20). The S/V ratio was fixed at 50 m^{-1}. Dissolved glass constituents Li and Cs were monitored as a function of time from few minutes to few days. The pH (25 °C) was 9.5.

2.2. Leachates and solids analysis

The solutions were analyzed by a PQ-Excel VG-Elemental ICP/MS for Li, Cs, Mo and Si, with a quantification limit of 0,1 ppb. The error was 3–5%. Prior to ICP/MS measurements, the solutions were filtered through 0.2 μm filters to remove potentially present glass particles. The leached glass samples were analyzed by a 8400 Shimadzu infrared spectroscope (FTIR) for concentration and speciation of water. The glass chips were analyzed directly after drying at 105 °C in an oven. Drying did not release the water from the hydrated de-alkalized glass. The powdered glass samples, were mixed after drying with KBr (about 6 mg of glass per100 mg of KBr) and cold pressed at 7.5 tons cm^{-2} to a pellet. A pellet of KBr was used as a blank to measure the water concentration sorbed onto the KBr. Water and silanol concentrations were determined according to Beer–Lambert law and taking the height of the band as described in the literature [27–29]. The molar extinction coefficient of water in the SON 68 was determined by calibrating the FTIR according to Nguyen et al.'s work [30]. The authors used a mixture of H_2O and D_2O (99.9%), resulting in the formation of three species: HOH, HOD and DOD. According to the reaction $H_2O + D_2O \rightarrow 2HOD$, one H_2O molecule splits into two HOD molecules and therefore the absorbance at 3400 cm^{-1}, due to the OH group, is proportional to the H_2O concentration.

Glass surface alteration products were analyzed using a JSM 5800 LV JEOL scanning electron microscope and ultra-thin sections of the glass/alteration layer interface of glass powders were analyzed by a HITACHI H900 NAR scanning transmission electron microscope. For both microscopes, the chemical analysis of the glass surface was obtained by EDS, with an estimated error not exceeding 5%.

In addition, X-ray reflectivity was used to measure the thickness and density of alteration layer formed on the glass surface upon alteration. A detailed description of the method is given in Rebiscoul et al. [31].

2.3. Modeling

Modeling of the experimental data was conducted with GM2001 model described in Grambow and Müller [19]. The model takes into consideration a de-alkalinized hydrated glass between the pristine glass and the alteration gel. In this layer, diffusion profiles, in opposite directions, exist for water molecules and alkali ions and boron. Some experimental parameters are fixed for all experiments at a given temperature: flow (0.014 L d^{-1}), solution volume (35 mL), silicon molality (4×10^{-3} or 8×10^{-3} mol kg^{-1}), silicon fraction retained in the

gel, gel porosity (20%), boron and lithium retention factors in the hydrated glass (100 and 10 kg m^{-3}). The GM2001 model application to experimental results is described by the fitting of water diffusion coefficient DH_2O. Experimental data are insensitive to effects of silica diffusion because silica transport through protective gel layers controls glass dissolution rates only if silica saturation is not reached, a condition which is avoided in the present study.

3. Results

3.1. Alteration kinetics

3.1.1. Static experiments

The dissolution rates from static tests were derived from the evolution of the measured Li and Cs concentrations in solution and not from B concentrations because of the high initial concentration in B in the synthetic solution. The dissolution rates NLR of the glass were calculated using the normalized mass loss NL(i) and the time interval Δt

$$\mathrm{NLR}(i) = (\Delta \mathrm{NL}(i))/\Delta t = \frac{\Delta \mathrm{NC}(i)}{(S/V)\Delta t} \quad (1)$$

with

NLR(i) dissolution rate in g m^{-2} d^{-1}
NL(i) normalized mass loss in g m^{-2}
NC normalized concentration in g m^{-3}
NC(i) $\frac{C_{\text{element}}}{\text{element weight fraction in pristine glass}}$
S/V glass surface area to volume of solution in m^{-1}

The dissolution rates are initially constant and decrease thereafter with time. The initial dissolution rates of the glass in solution are plotted in Fig. 1 as a function of Si-solution concentration in the leachant. The data are average values for Cs and Li measurements. Errors are about 10%. The figure shows that the dissolution rate decreases with increasing Si-concentration. The rates are 0.89, 0.5 and 0.37 g m^{-2} d^{-1} for Si-concentration of 0, 24 and 48 ppm, respectively. For Si-concentration between 96 and 240 ppm (data are only shown up to 120 ppm Si) the dissolution rate remained independent of the Si concentration at a low value of about 0.04 g m^{-2} d^{-1}. From this diagram one can deduce that the saturation concentration of Si is about 70 ppm at pH 9.5. In case of initial silicon concentrations higher than this saturation value, the reaction rates were about a factor 20 lower than the rates in the initial absence of dissolved silica. These results support the hypothesis that the synthetic solution with a Si-concentration of 120 ppm can be used to represent (super-)saturation conditions.

3.1.2. Dynamic experiments

In the dynamic experiments, the normalized dissolution rate was calculated according to the following expression:

$$\mathrm{NLR}_{i+1} = \frac{\left(\frac{\mathrm{NC}_i - \mathrm{NC}_{i+1}}{((t_{i+1}) - t_i)}\right) + \left(\frac{F}{V} \times \mathrm{NC}_{i+1}\right)}{\frac{S}{V}}, \quad (2)$$

NC normalized concentration in g m^{-3}
F alteration solution flow in L d^{-1}
V solution volume in L

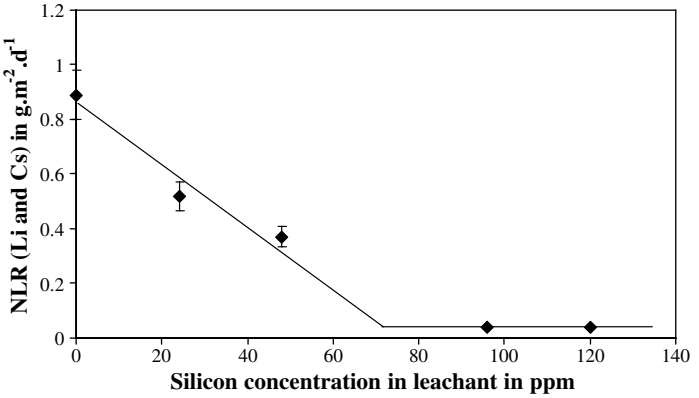

Fig. 1. Dissolution rates in g m^{-2} d^{-1} as a function of silicon concentration in ppm during alteration in a static system at 90 °C with a solution enriched in sodium and boron and at pH 9.5.

S SON 68 glass surface area in m^2
t alteration time in d
i and $i+1$ denote two consecutive sampling intervals

The results of dynamic experiments at 50 or 90 °C at various pH values are given in Fig. 2(a)–(c). The figures show the normalized dissolution rates of the glass as a function of time. Regardless the temperature and pH, the release of Li and Cs seems to follow similar trends indicating release control by a similar process. The release of these elements follows a slope of $-1/2$ in double logarithmic diagrams suggesting release control by a diffusion process. This result is in agreement with literature data on glasses alteration showing the increase of alkali concentration in solution as a function of square root of time [32–36]. At the end of experiments with powders, dissolution rates measured by Li and Cs were about 10^{-3} g m^2 d^{-1}.

For experiments conducted with glass chips, dissolution rates measured by Li and Cs are higher

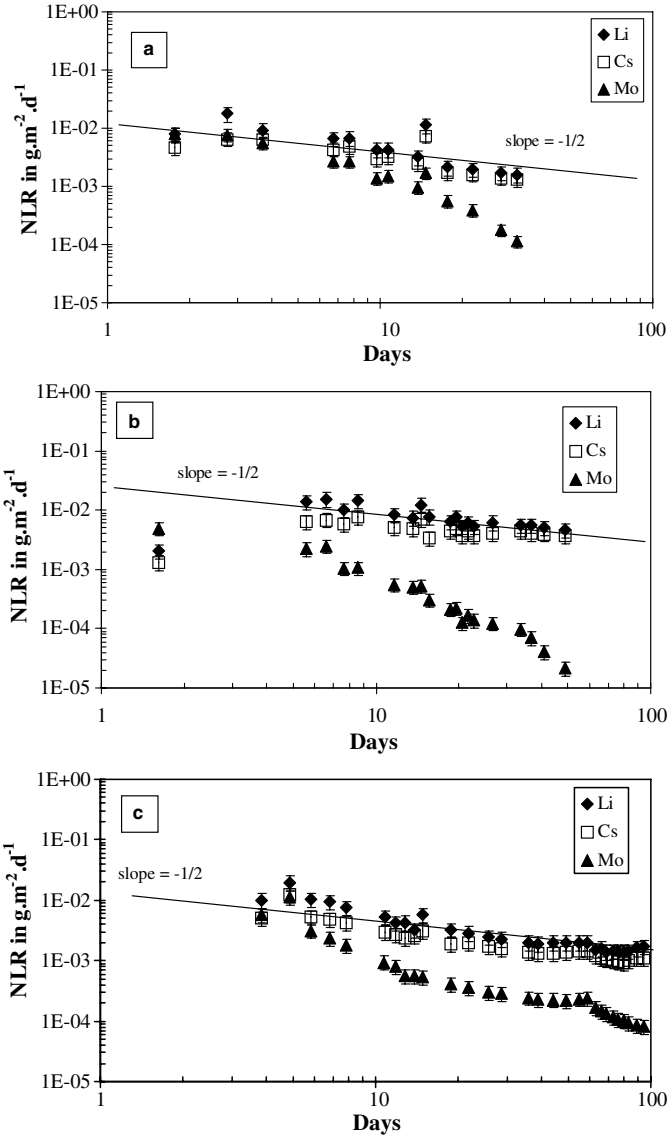

Fig. 2. (a) Normalized dissolution rates for SON 68 glass powder (d20) alteration in a dynamic system at 50 °C with a synthetic solution at initial pH 7.2. (b) Normalized dissolution rates for SON 68 glass powder (d5) alteration in a dynamic system at 90 °C with a synthetic solution at initial pH 4.8. (c) Normalized dissolution rates for SON 68 glass powder (d5) alteration in a dynamic system at 90 °C with a synthetic solution at initial pH 9.8 (silicon = 240 ppm).

than those for experiments with powders. This may be due to an underestimation of the calculated surface area due to bubbles formation during glass synthesis and polishing defects.

Tables 2 and 3 summarize for Si concentrations of 120 and 240 ppm respectively the normalized dissolution rates for Li, Cs and Mo obtained at the end of the experiments as a function of pH, temperature and sample type. The normalized dissolution rates for Li and Cs are quite similar and are between 10^{-2} and 10^{-3} g m^{-2} d^{-1}. Dissolution rates for Mo are between 10^{-4} and 10^{-5} g m^{-2} d^{-1}. The normalized Mo release rates are similar to long-term dissolution rates obtained with boron as a tracer for SON 68 glass alteration in de-ionized water at 90 °C ([12], Curti, personal communication). One may conclude that the release rate data for Mo may represent glass matrix dissolution rate as suggested by McGrail et al. [20]. Hyatt et al. [37] have also demonstrated that Mo dissolution rates were similar to Na and B dissolution rates from Magnox wastes glasses when alkali molybdate is completely soluble in glass. ESR, XAS and EXAF were used to determine that $[MoO_4]^{2-}$ species did not form part of the polymeric glass network in Magnox glasses, they were like encapsulated with network modifier rich cavities defined by the borosilicate glass network. However, it cannot be excluded that Mo concentrations are controlled by solubility constraints of phases such as $CaMoO_4$ since solutions were calculated to be supersaturated with respect to this phase.

Li, Cs and Mo release rates are similar from experiments with 120 and 240 ppm of silicon.

Table 3
SON 68 glass normalized dissolution rates in (g_{glass} m^{-2} d^{-1}) obtained in a dynamic system at 90 °C with a synthetic solution (silicon = 240 ppm) at initial pH 4.8, 7.2 and 9.8

Temperature = 90 °C				Element
Initial pH	4.8	7.2	9.8	
d20	10^{-2}	5×10^{-3}	2×10^{-3}	Li
	10^{-2}	5×10^{-3}	2×10^{-3}	Cs
	10^{-4}	7×10^{-4}	2×10^{-4}	Mo

3.2. Modeling

Examples of modeling results with GM2001 model are plotted in Figs. 3 and 4. The figures show a comparison of experimental data with results of simulation obtained with powder (d5) and a glass chip at 50 °C with a solution concentration of 120 ppm of Si and initial pH 4.8. The apparent water diffusion coefficients fitted from the experimental results at 50 and 90 °C are given in Tables 4 and 5 for solutions containing 120 and 240 ppm of silicon respectively at initial pH 4.8, 7.2 or 9.8. Water diffusion coefficients were found to be between 10^{-18} and 10^{-24} m^2 s^{-1}. This corresponds to solid-state ion diffusion coefficients in minerals [38]. For a given pH and temperature, a similarity is observed between water diffusion coefficients determined for experiments using d20 and d5. No effect of the degree of supersaturation of Si (120 vs. 240 ppm) on apparent water diffusion coefficients was observed. Water diffusion coefficients are higher at 90 °C than at 50 °C and increase with decreasing pH. At low pH, the significant formation of silanol groups is supposed to contribute to a

Table 2
Normalized Mo, Li and B dissolution rates in (g_{glass} m^{-2} d^{-1}) from SON 68 glass obtained at the end of experiments with the powdered glass samples d5 and d20 and a glass chip conducted in a dynamic dissolution test at 50 or 90 °C with a synthetic solution at initial pH 4.8, 7.2 and 9.8 (silicon = 120 ppm)

Temperature	50 °C			90 °C			Elements
Initial pH	4.8	7.2	9.8	4.8	7.2	9.8	
d20	2×10^{-3}	2×10^{-3}	7×10^{-5}	5×10^{-3}	2×10^{-3}	2×10^{-3}	Li
	2×10^{-3}	2×10^{-3}	2×10^{-4}	5×10^{-3}	2×10^{-3}	6×10^{-4}	Cs
	3×10^{-5}	10^{-4}	4×10^{-5}	2×10^{-5}	10^{-4}	2×10^{-4}	Mo
d5	10^{-3}	10^{-3}	–[a]	4×10^{-3}	10^{-3}	10^{-3}	Li
	10^{-3}	10^{-3}	–[a]	4×10^{-3}	10^{-3}	10^{-4}	Cs
	10^{-5}	10^{-4}	–[a]	2×10^{-5}	10^{-4}	10^{-4}	Mo
Chip	3×10^{-3}	3×10^{-3}	4×10^{-4}	4×10^{-2}	5×10^{-3}	10^{-2}	Li
	3×10^{-3}	10^{-3}	10^{-4}	4×10^{-2}	6×10^{-3}	8×10^{-3}	Cs
	10^{-4}	5×10^{-3}	10^{-4}	10^{-3}	4×10^{-4}	10^{-3}	Mo

[a] Not realized.

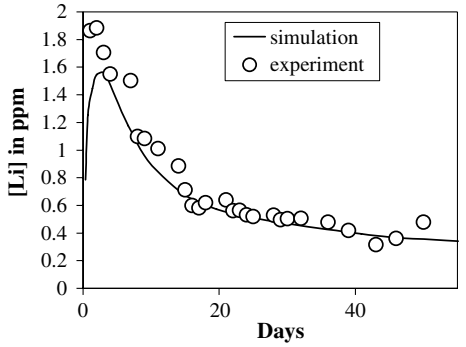

Fig. 3. Comparison of experimental data with simulations using the GM2001 model for SON 68 glass powder d5 alteration conducted in a dynamic system at 50 °C with a synthetic solution at initial pH 4.8.

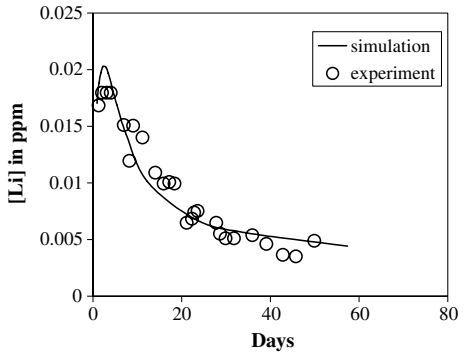

Fig. 4. Comparison of experimental data with simulations using the GM2001 model for SON 68 glass chip alteration conducted in a dynamic system at 50 °C with a synthetic solution at initial pH 4.8.

more opened structure of the hydrated glass surface region, which favors the diffusion of water.

A comparison of water diffusion coefficients in the glass obtained in the present study with those from the literature for a variety of natural and synthetic silicate glasses is given in Fig. 5. The figure shows that our data with the SON 68 glass correlate well with the rest despite of differences in experimental conditions described in the literature [39–47]. Certain experiments reported in the literature were conducted at higher temperatures (up to 200 °C) and with very simple composition compared to the SON 68 glass. Water diffusion coefficients determined are similar to those found by Doremus [1] and Lanford et al. [4], who studied the alteration of LiO_2–SiO_2 and Na_2O–CaO–SiO_2 glasses at 50 and 90 °C in water. This supports our interpretation of glass dissolution data under Si supersaturated conditions by a water diffusion mechanism.

Table 5
Water diffusion coefficients in $m^2\ s^{-1}$ obtained with experimental data modeling of SON 68 glass alteration in a dynamic system at 90 °C with a synthetic solution containing 240 ppm Si at initial pH 4.8, 7.2 and 9.8

Temperature = 90 °C			
Initial pH	4.8	7.2	9.8
d20	5×10^{-21}	6×10^{-22}	2×10^{-22}
d5	2×10^{-21}	6×10^{-22}	10^{-22}

The activation energies calculated from the water diffusion coefficients in the SON 68 glass are given in Fig. 6. The activation energies are 49, 52 and 85 kJ mol^{-1} for experiments conducted with glass powder (d20) at initial pH 4.8, 7.2 and 9.8, respectively. These values are similar to the value of 60 kJ mol^{-1} given by Delage [48], for hydrolysis controlled initial SON 68 glass dissolution. This suggests a similar process governing water diffusion and glass hydrolysis.

3.3. Surface analysis by FTIR

3.3.1. FTIR calibration

The results of FTIR calibration with a mixture of D_2O–H_2O are plotted in Fig. 7. A deviation of Beer–Lambert law linearity is observed for H_2O concentration higher than 12%. The molar extinction coefficient of water is 88 L mol^{-1} cm^{-1}. This value is similar to that obtained by Geotti-Blanchini

Table 4
Water diffusion coefficients in $m^2\ s^{-1}$ obtained with experimental data modeling of SON 68 glass alteration in a dynamic system at 50 or 90 °C with a synthetic solution containing 120 ppm Si at initial pH 4.8, 7.2 and 9.8

Temperature	50 °C			90 °C		
Initial pH	4.8	7.2	9.8	4.8	7.2	9.8
d20	4×10^{-22}	6×10^{-23}	3×10^{-24}	3×10^{-21}	5×10^{-22}	10^{-22}
d5	8×10^{-23}	5.3×10^{-23}	–	10^{-21}	1.5×10^{-22}	6×10^{-23}
Chip	2.5×10^{-21}	1.5×10^{-22}	–	8×10^{-19}	4×10^{-21}	2×10^{-21}

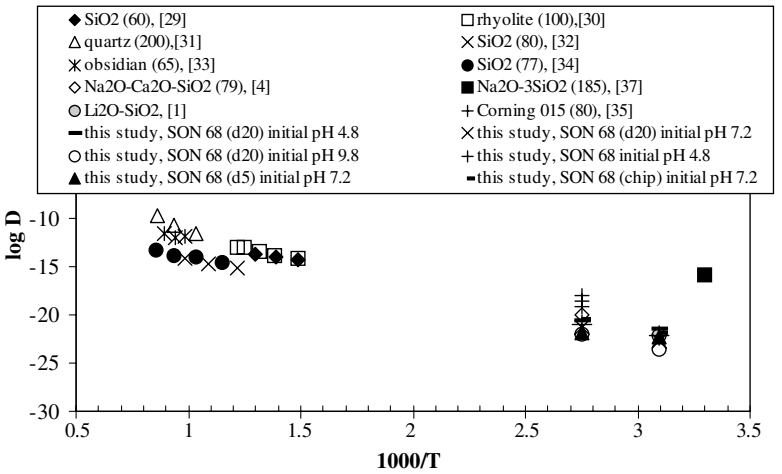

Fig. 5. Arrhenius diagram: $\mathrm{Log}\,DH_3O^+$ or $\log DH_2O$ ($m^2\,s^{-1}$) as a function of ($1000/T$).

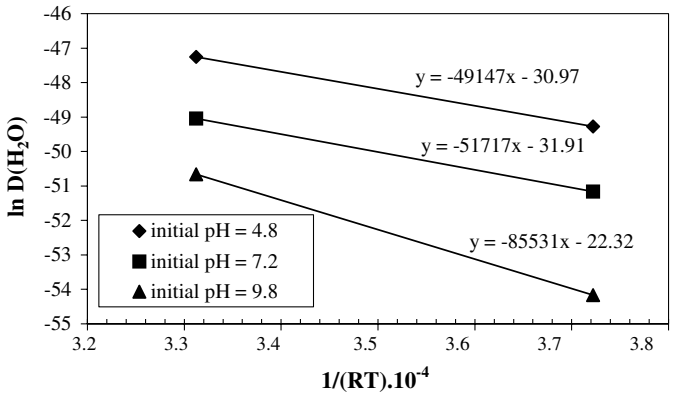

Fig. 6. $\mathrm{Ln}\,DH_2O$ ($m^2\,s^{-1}$) as a function of $(1/RT)\times 10^{-4}$determined from SON 68 glass powder d20 alteration conducted in a dynamic system with a synthetic solution at initial pH 4.8, 7.2 or 9.8. The slopes of the lines correspond to the activation energies ($J\,mol^{-1}$ of SON 68 glass).

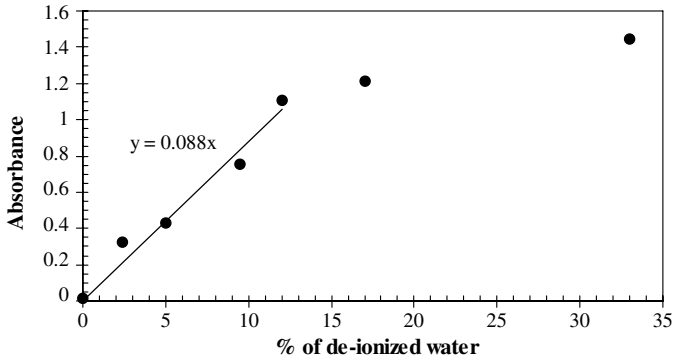

Fig. 7. FTIR calibration for water measurement: absorbance as a function of the quantity of H_2O.

et al. [49] for soda-lime silicate glasses. To quantify silanol concentrations in the glass samples, no calibration was performed, instead, a molar extinction coefficient from the literature was used [39].

3.3.2. Spectra analysis

For water speciation a Gaussian deconvolution of the spectra was applied, attributing the bands according to the work of Davis and Tomozawa [50]. An example of a measured and deconvoluted spectrum for the 14 days experiment of glass powder altered in synthetic solution at initial pH 4.8 is given in Fig. 8. The band near 3200 cm^{-1} is attributed to molecular water in interstitial sites, which vibrates freely and to molecular water, which is hydrogen-bonded to the silanol group. This band is noted H_2O_I. The band near 3425 cm^{-1} is due to the contribution of the H_2O_I band and to molecular water which is directly connected to the network as described by Dunken's mechanism [51]. This band is noted $H_2O_{I\&II}$ and is used for water quantification. Silanol groups vibrate near 3570 cm^{-1}. The application of the Beer–Lambert law to data given in Fig. 7 had led to the concentration of molecular water and silanol groups (Fig. 9). In all experiments, water concentrations are higher than silanol concentrations. About 80% of the hydrogen contained in the altered glass is present as molecular water and 20% as silanol groups. The glass hydration increases with temperature. Hence, at 90 °C, water and silanol concentrations are higher than at 50 °C. Moreover, for a given temperature, the water and silanol concentrations in the glass increase with decreasing pH, even though the concentration ratio of water to silanol stays constant. No effect of the Si-concentration on glass hydration was observed when varying dissolved silicon concentration

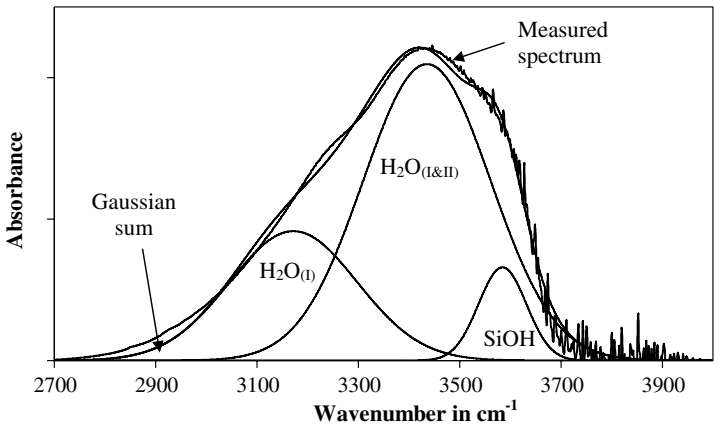

Fig. 8. Measured and deconvoluted FTIR spectra obtained after 14 days of SON 68 glass powder alteration with a synthetic solution at initial pH 4.8.

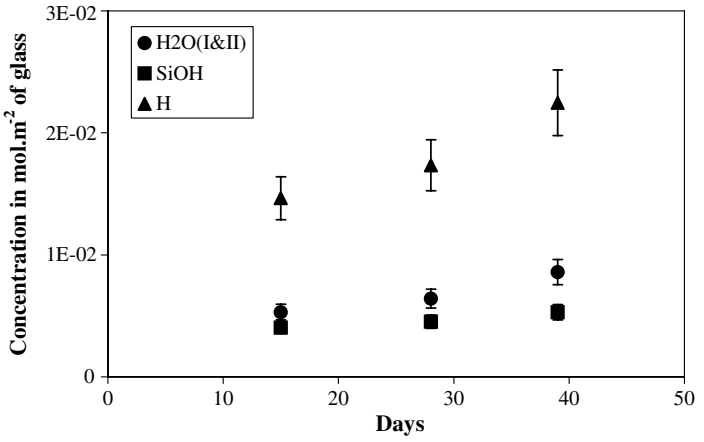

Fig. 9. Water, silanol and hydrogen concentrations in mol m^{-2} of SON 68 glass chip altered for 39 days in a dynamic system at 90 °C with a synthetic solution at initial pH 7.2.

between 120 and 240 ppm. In these experiments, the absorbances of H_2O and SiOH are quite similar (Table 6). It should be mentioned that the term 'water and silanol concentration' is somehow misleading. It applies in the context of the present analyses not to the hydrated fraction of the glass but to the total glass sample. Hence, the progress glass hydration leads to increased water 'concentration' in the glass, even though the water content of the hydrated fraction of the glass might remain constant.

Based on the ICP/MS solution analysis and FTIR glass analysis, a ratio of H-uptake to ($Li^+ + Cs^+ + Na^+$) release equal to 2.6 ± 0.3 is determined as indicated in Fig. 10 for experiment conducted with the SON 68 glass at 90 °C and Si-concentration of 120 ppm. A similar ratio was obtained for the glass altered at 50 and at 90 °C regardless the Si-concentration (120 or 240 ppm) and solution pH, indicating a similar mechanism of glass alteration. This indicates that the composition of the hydrated glass is in first approximation independent of reaction progress, solution pH, temperature and degree of supersaturation. Also, a ratio of H (uptake)/Na (release) near to 3 was obtained by several authors from silicate glasses measured by nuclear analysis [2,4,5,52,6,53].

Table 6
Absorbances of H_2O and SiOH obtained during SON 68 glass powder d20 alteration in a dynamic system with a synthetic solution at initial pH 4.8

[Si] in ppm	Days	Absorbance	
		H_2O	SiOH
120	14	0.419	0.132
	29	0.694	0.217
	47	0.812	0.244
240	14	0.409	0.106
	28	0.736	0.201
	41	0.913	0.203

3.4. Surface analysis by electron microscopy

In most experiments, in particular at 50 °C, the glass surface observation with scanning electron microscope did not show any secondary phases. This can also be seen in Fig. 11 obtained from a glass chip altered for 37 days in the synthetic solution with 120 ppm Si at 90 °C. Only at 90 °C some alteration products were observed. At an initial

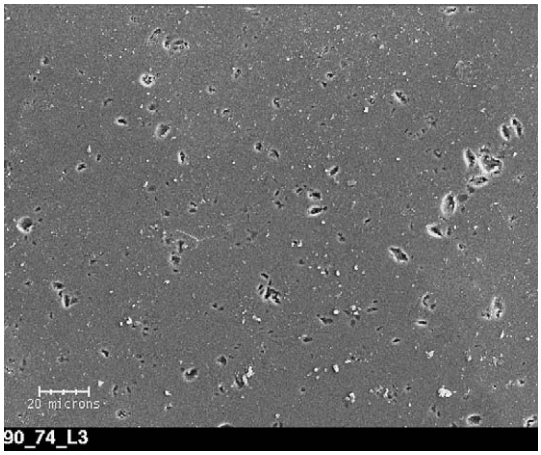

Fig. 11. SEM photograph of the SON 68 glass chip. The glass was altered for 37 days in a dynamic system at 90 °C with a synthetic solution at initial pH 7.2.

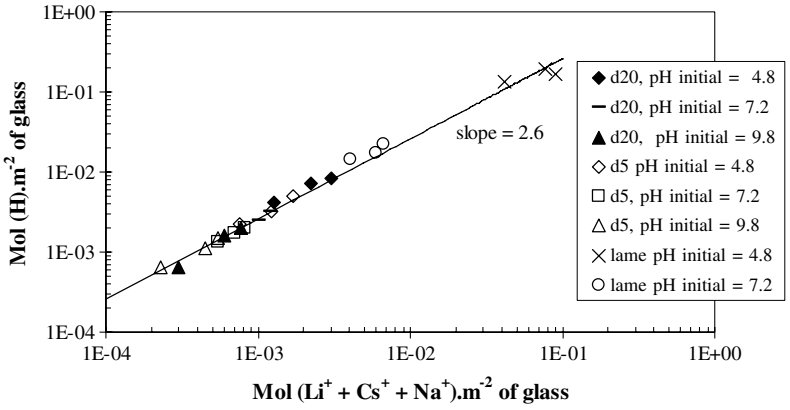

Fig. 10. Hydrogen concentration in mol m^{-2} of altered SON 68 glass as a function of total alkalis released from the glass (Li^+, Cs^+, Na^+) in mol m^{-2} for experiments conducted in a dynamic system at 90 °C with a synthetic solution.

pH of 4.8 a gel layer can be observed after 47 days of alteration (Fig. 12). At 90 °C and initial pH 9.8 rare phyllosilicates were observed within 56 days. EDS analysis of the gel layer shown in Fig. 12 is given in Table 7. The gel is enriched in Si and Al, compared to the pristine glass, and has lost most of its Na, as a result of ion exchange with protons, as often reported in glass alteration studies [54–56].

Detailed analyses of the gel layer were conducted on ultra-thin sections under the transmission electron microscope. Samples from experiments with glass powder (d5) conducted at 90 °C and pH 4.8 or 9.8 were studied. An alteration gel is observed at pH 4.8 with a thickness less than 100 nm (Fig. 13). The chemical composition of the gel is similar to that obtained by SEM with an enrichment in Zr and Mo and an important depletion in Na.

3.5. Surface analysis by X-ray reflectivity

The results of X-ray reflectivity of a glass chip altered at 90 °C in synthetic solution with 120 ppm Si and pH 9.8 are shown in Fig. 14. Also, the figure contains the results of simulation. The values obtained for roughness, thickness and density are indicated in Table 8. A high density layer with no gradient is observed indicating, that under our experimental conditions, the altered surface is likely a hydrated glass formed by ionic-exchange with alkalis and water. The measured thickness of 52 nm is similar to that obtained from Li-concentrations (63 nm). The densities of the two glass faces (2.21 and 2.32) are lower than that measured from the pristine glass ($d = 2.63$). This is due to low density of water replacing the alkalis in the glass. However, the densities are much higher than those reported for dense gel layers on glasses as reported by Rebiscoul et al. [31]. This confirms that the principal alteration process observed in our study is glass hydration and not gel layer formation.

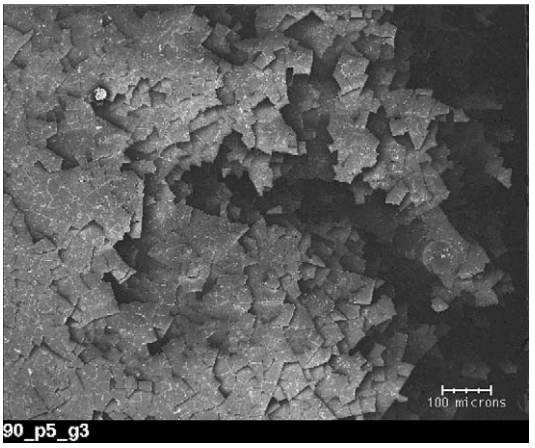

Fig. 12. SEM photograph of the SON 68 glass chip showing a gel layer. The glass was altered for 47 days in a dynamic system at 90 °C and pH 4.8.

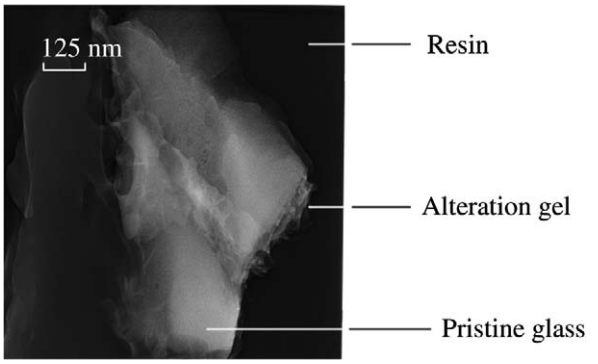

Fig. 13. Alteration gel observed by STEM on glass powder (d5) altered in a dynamic system at 90 °C with a synthetic solution at initial pH 4.8.

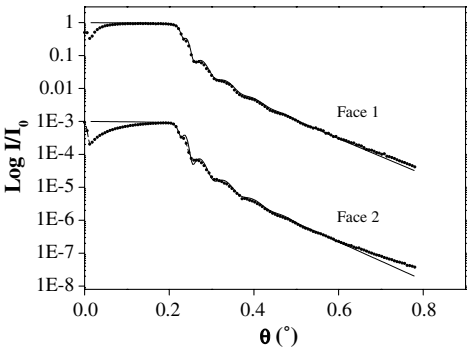

Fig. 14. Experimental and simulation curves obtained by X-ray reflectivity on SON 68 glass chip altered during 57 days in a dynamic system at 90 °C with a synthetic solution at initial pH 9.8.

Table 7
Composition in at.% of the alteration gel and the pristine glass by SEM

Element	Si	Al	Na	Zr	Mo	Fe	O	Ca
Alteration gel	23.48	3.10	3.15	0.68	0.41	1.04	68.13	
Pristine glass	18.68	2.44	8.63	0.55	0.34	1.10	66.48	1.82

Table 8
Roughness, thickness and density obtained with X-ray reflectivity on SON 68 glass chip altered during 57 days in a dynamic system at 90 °C with a solution at initial pH 9.8

Chip	Layer			Substrate	
	Roughness (nm)	Thickness (nm)	Density (g cm^{-3})	Roughness (nm)	Density (g cm^{-3})
Face 1	1.5 ± 0.1	52 ± 1	2.32 ± 0.02	4.0 ± 0.1	2.63 ± 0.02
Face 2	1.6 ± 0.1	52 ± 1	2.21 ± 0.02	4.0 ± 0.1	2.63 ± 0.02

4. Discussion

The mechanism of glass hydration can be described by several models [1–3,45]. Depending on the H/Na ratio, some models describe the glass hydration as simple ionic-exchange between protons or hydronium and alkalis [1], while others suggest ionic-exchange H^+–Na^+ followed by migration of molecular water in the resulting pores [2] or water diffusion followed by network hydrolysis and Na^+ and OH^- release [47]. In addition, Ernsberger [3] suggested the simultaneous diffusion of H_3O^+ and water molecules supported by a H/Na ratio higher than 3. Therefore, depending on the model the limiting step is either the water diffusion or diffusivity of exchangeable ions. In the present study the H/Na ratio of 2.6 suggests a complex hydration mechanism that might include ionic-exchange, water diffusion and network hydrolysis. In the experiments at pH 9.8, surface analyses by transmission electron microscopy did not reveal any porosity in the glass surface. This suggests that in these experiments glass alteration is mainly dominated by ionic-exchange and water diffusion, leading to a dense hydrated glass. In agreement with a first order dissolution rate law, network hydrolysis/dissolution is less important or absent due to high initial Si-concentration in synthetic solution.

An attempt was made to calculate mass, charge and volume balance during the glass alteration using a simplified formula of the SON 68 glass. Using the compositional ratios of the glass composition given in Table 1 and fixing SiO_2 with a stoichiometric number of 1, a simplified molar composition of the glass can be written as

$$(SiO_2)_1\,(B_2O_3)_{0.266}\,(Li_2O, Cs_2O, Na_2O)_{0.304}\,(\text{other oxides})_{0.381} \quad (3)$$

The studies of the SON 68 glass structure suggest that B exists as a mixture of tetragonal and trigonal form [57–60]. The tetragonal boron represents near 70% of total B [61] and the formula in the glass can be expressed as reedmergnerite, $NaBSi_3O_8$. The trigonal B can be written as B_2O_3. The formula given in (3) can then be written as

$$(NaBSi_3O_8)_{0.33}\,(B_2O_3)_{0.1}\,(Na_2O)_{0.139}\,(\text{other oxides})_{0.381} \quad (4)$$

The reactions of each oxide with water can be written as (5) for B_2O_3 (6) for reedmergnerite and (7) for Na_2O

$$0.1[(B_2O_3)_{glass} + 6H_2O \rightarrow 2(H_3BO_3)_{solution} + (3H_2O)_{glass}] \quad (5)$$

This reaction leads to the formation of boric acid in solution. Given that the reaction is isovolumic and the ionic radius of B can be neglected with regard that of O, this implies that each boron oxide is replaced by 3 water molecules in the glass

$$0.33[(NaBSi_3O_8)_{glass} + 3.26(H_2O)_{solution} \rightarrow (Na^+, OH^-)_{solution} + (H_3BO_3)_{solution} + 2.5(SiO_2)_{glass} + 0.5(H_2SiO_3)_{glass} + 0.76(H_2O)_{glass}] \quad (6)$$

Reaction (6) shows that the reaction of water with reedmergnerite leads to the formation Na^+, OH^- and boric acid. A fraction of water in the glass is present as silanol groups in the H_2SiO_3 form

$$0.143[(Na_2O)_{glass} + 2.52(H_2O)_{solution} \rightarrow 2(Na^+, OH^-)_{solution} + 1.52(H_2O)_{glass}] \quad (7)$$

Reaction (7) leads to the formation of Na^+, OH^- and water in the glass. The reaction is isovolumic and the coefficient 1.52 corresponds to the molar volume ratio of Na_2O/H_2O.

The global reaction of the glass alteration is given in (8)

$$[(B_2O_3)_{0.1}\,(NaBSi_3O_8)_{0.33}\,(Na_2O)_{0.143}]_{glass} + 2.036(H_2O)_{solution} \rightarrow [(Na^+, OH^-)_{0.616}\,(H_3BO_3)_{0.53}]_{solution}\,[(SiO_2)_{0.825}\,(H_2SiO_3)_{0.165}\,(H_2O)_{0.768}]_{glass} \quad (8)$$

This global reaction gives a H/Na ratio of 3.02, near to that obtained experimentally (2.6). Also, the water in the glass is present as 82% of molecular water and 18% as SiOH, in good agreement with FTIR data giving a value of 80% H_2O and 20% SiOH. We calculated a density of hydrated glass supposing a isovolumic reaction. The obtained value is $d_{\text{hydrated glass}} = 2.17\ \text{g cm}^{-3}$. This density is near to that measured by X-ray reflectivity.

5. Conclusions

1. The use of synthetic solutions with compositions derived from glass alteration experiments can successfully simulate continued glass alteration under Si saturation conditions. In addition, dynamic experiments prevented substantial secondary phases precipitations. The procedure applied in this work offered the flexibility necessary to cover a wide range of experimental conditions.
2. A diffusion process controls the release of alkalis from the glass. The final SON 68 glass dissolution rate at 90 °C calculated with Mo data is in the order of $10^{-4}\ \text{g m}^{-2}\ \text{d}^{-1}$. The first order dissolution rate law has been validated for Si concentrations lower than the saturation concentration. However, at Si concentrations higher than the apparent saturation concentration, glass alteration continues with a low rate.
3. Under saturated or supersaturated conditions, the low residual dissolution rate of the glass is due the to low diffusion coefficients of water in the SON 68 glass. These diffusion coefficients were derived with the GM2001 model using glass alteration experimental data and ranged between 10^{-18} and $10^{-24}\ \text{m}^2\ \text{s}^{-1}$. At pH 9.8, relevant to nuclear waste disposal, the water diffusion coefficients are between 2×10^{-21} and $6 \times 10^{-23}\ \text{m}^2\ \text{s}^{-1}$. The calculated activation energies are between 50 and 80 kJ mol^{-1}.
4. The obtained water diffusion coefficients and activation energies were similar for nuclear waste glass, for alkali silicate glass and for obsidian.
5. For the first time, water quantification and speciation in the SON 68 glass were determined by FTIR. The water speciation remained unchanged regardless the experimental conditions with 80% of water in the glass present as molecular water and 20% as silanol groups. This implies a similar mechanism of glass alteration.
6. The quantity of water molecules entering the glass is directly proportional to the release of alkali ions. Combination of results of solution analysis for alkalis release and glass surface analysis for water allowed to determine a ratio of H to alkalis of 2.6 ± 0.3. Similar results were obtained by mass, charge and volume balance.

6. Implications for nuclear waste glass disposal

The present work shows that under the silicon saturation conditions expected to prevail in a disposal vault, water diffusion may play an essential role in glass alteration. Under disposal conditions, where the groundwater flow is supposed to be low, dilution effect of saturated solution resulting from glass/groundwater interaction remains minor. Under these conditions, a pure affinity rate law or a rate law based on silicon transport through a gel layer cannot explain our data since these rate laws alone would yield dissolution rates of zero. Our experimental data can only be used in overall glass performance assessment if water diffusion is coupled to the affinity law in the modeling. However, this does not suggest that our data can directly be applied to a disposal conditions. Already after few years the diffusion of water molecules in the glass becomes very slow, and its contribution to the long-term release of radionuclides from glass will be low under open systems conditions. Nevertheless, if this process is ignored in the evaluation of experimental glass/water reaction data, erroneous parameters for long-term prediction are obtained. Hence, understanding of the role of water diffusion is a prerequisite of long-term glass performance predictions.

Acknowledgements

We would like to thank P. Jollivet and D. Rebiscoul from CEA-VALRHO (Marcoule, France) for providing the SON 68 glass and for realizing X-ray reflectivity analysis. Also a special thank to G. Morvan for ultra-thin sections preparation and to A. Barreau and E. Gautier from the Institut des Matériaux de Nantes Jean Rouxel (Nantes, France) for electron microscopy studies. We are also grateful to S. Delaunay and B. Cahingt for ICP/MS analysis.

References

[1] R.H. Doremus, J. Non-Cryst. Solids 19 (1975) 137.
[2] I.S.T. Tsong, C.A. Houser, W.B. White, A.L. Wintenberg, P.D. Miller, C.D. Moak, Appl. Phys. Lett. 39 (8) (1981) 669.

[3] F.M. Ernsberger, collected papers, in: International Congress on Glass, 1986, p. 319.
[4] W.A. Lanford, K. Davis, P. Lamarche, T. Laursen, R. Groleau, R.H. Doremus, J. Non-Cryst. Solids 33 (1979) 249.
[5] B.C. Bunker, G.W. Arnold, E.K. Beauchamp, D.E. Day, J. Non-Cryst. Solids 58 (1983) 295.
[6] J.C. Dran, G. Della Mea, A. Paccagnella, J.C. Petit, L. Trotignon, Phys. Chem. Glasses 29 (1988) 249.
[7] J.L. Noguès, Thesis, Université de Montpellier, 1984.
[8] H. Charpentier, Note Technique SEM no. 30/87 du CEA, IRDI/DMECN, DMG-SEM.LECM, 1987.
[9] A. Abdelouas, J.L. Crovisier, W. Lutze, B. Fritz, A. Mosser, R. Müller, Clays Clay Miner. 42 (1994) 526.
[10] E. Vernaz, S. Gin, C. Jégou, I. Ribet, J. Nucl. Mater. 298 (2001) 27.
[11] C. Jégou, S. Gin, F. Larché, J. Nucl. Mater. 280 (2000) 216.
[12] C. Jégou, Thesis, Université de Montpellier II, 1998.
[13] S. Gin, Sci. Basis Nucl. Manage. 663 (2000) 207.
[14] S. Gin, I. Ribet, M. Couillard, Mater. Res. Soc. Symp. Proc. 198 (2001) 1.
[15] B. Grambow, Sci. Basis Nucl. Manage. 44 (1985) 15.
[16] W.L. Bourcier, D. Peiffer, K.G. Knauss, K.D. MsKeegan, D.K. Smith, Sci. Basis Nucl. Manage. 176 (1990) 209.
[17] P.K. Abraitis, B.P. McGrail, B.P. Trivedi, Sci. Basis Nucl. Manage. 556 (1999) 401.
[18] T. Advocat, J.L. Chouchan, J.L. Crovisier, C. Guy, V. Daux, C. Jégou, S. Gin, E. Vernaz, Sci. Basis Nucl. Manage. 506 (1998) 63.
[19] B. Grambow, R. Müller, J. Nucl. Mater. 298 (2001) 112.
[20] B.P. McGrail et al., PNNL report 2001 for US Department of Energy.
[21] J. Sheng, S. Luo, B. Tang, Nucl. Tech. 123 (1998) 296.
[22] Y. Chen, B.P. McGrail, D.W. Engel, Mater. Res. Soc. Symp. Proc. 465 (1997) 1051.
[23] I. Tovena, Thesis, Université de Montpellier II, 1995.
[24] P. Van Iseghem, B. Grambow, Mater. Res. Soc. Symp. Proc. 112 (1988) 691.
[25] J. Patyn, P. Van Iseghem, W. Timmermans, Mater. Res. Soc. Symp. Proc. 176 (1990) 299.
[26] P. Jollivet, Y. Minet, M. Nicolas, E. Vernaz, J. Nucl. Mater. 281 (2000) 231.
[27] S. Newman, E.M. Stolper, S. Epstein, Am. Miner. 71 (1986) 1527.
[28] E. Stolper, Contribution Mineral. Petrol. 81 (1982) 1.
[29] Y. Zhang, R. Belcher, P.D. Ihinger, L. Wang, Z. Xu, S. Newman, Geochim. Cosmochim. Acta 61 (15) (1997) 3089.
[30] T. Nguyen, E. Byrd, D. Bentz, J. Adhesion 48 (1995) 169.
[31] D. Rebiscoul, A. Van der lee, F. Rieutord, F. Né, O. Spalla, A. El-mansouri, P. Frugier, A. Ayral, S. Gin, J. Nucl. Mater. (2004).
[32] M.A. Rana, R.W. Douglas, Phys. Chem. Glasses 2 (1961) 179.
[33] B.C. Bunker, Mater. Res. Soc. Symp. Proc. 84 (1987) 493.
[34] J.C. Petit, G. Della Mea, J.C. Dran, M.C. Magonthier, P.A. Mando, A. Paccagnella, Geochim. Cosmochim. Acta 54 (1990) 1941.
[35] Z. Boksay, G. Bouquet, S. Dobos, Phys. Chem. Glasses 9 (1968) 69.
[36] L.L. Hench, D.E. Clark, J. Non-Cryst. Solids 28 (1978) 83.
[37] N.C. Hyatt, R.J. Short, R.J. Hand, W.E. Lee, F. Livens, J.M. Charnock, R.L. Bilsborrow, The Structural Chemistry of Molybdenum in Model High Level Nuclear Waste Glases investigated by Mo K-edge X-ray Absorption Spectroscopy, vol. 168, American Ceramic Society, 2004, p. 179.
[38] D.M. Strachan, R.P. Turcotte, B.O. Barnes, Radioactive Waste Manage. – Nucl. Technol. 56 (1982) 306.
[39] N. Yanagisawa, K. Fujimoto, S. Nakashima, Y. Kurata, N. Sanada, Geochim. Cosmochim. Acta 61 (6) (1997) 1165.
[40] Y. Zhang, E.M. Stolper, G.J. Wassenberg, Geochim. Cosmochim. Acta 55 (1991) 441.
[41] A.K. Kronenberg, S.H. Kirby, R.D. Aines, G.R. Rossman, J. Geophys. Res. 91 (1986) 12723.
[42] H. Wakabayashi, M. Tomozawa, J. Am. Ceram. Soc. 72 (1989) 1850.
[43] H.R. Shaw, J. Geophys. Res. 68 (1963) 6337.
[44] A.J. Moulson, J.P. Roberts, J. Chem. Soc. Faraday Trans. 57 (1960) 1208.
[45] R.H. Doremus, Y. Mehrota, W.A. Lanford, C. Burman, J. Nucl. Mater. 18 (1983) 612.
[46] C.A. Houser, J.S. Herman, I.S.T. Tsong, W.B. White, W.A. Lanford, J. Non-Cryst. Solids 41 (1980) 89.
[47] B.M.J. Smets, T.P.A. Lommen, J. Phys. Chem. 43 (9) (1981) 649.
[48] F. Delage, Thesis, Université de Montpellier II, 1992.
[49] F. Geotti-Bianchini, H. Geibler, F. Kramer, I.H. Smith, Glastech. Ber. Glass Sci. Technol. 72 (4) (1999) 103.
[50] K.M. Davis, M. Tomozawa, J. Non-Cryst. Solids 201 (1996) 177.
[51] H.H. DunkenTreatise on Materials Science and Technology, vol. 22, Academic Press, New York, 1982, p. 1.
[52] K.H. Schnatter, R.H. Doremus, J. Non-Cryst. Solids 102 (1988) 11.
[53] B.C. Bunker, D.R. Tallant, T.J. Headley, G.L. Turner, R.J. Kirkpatrick, Phys. Chem. Glasses 29 (3) (1988) 106.
[54] J.L. Crovisier, J.P. Eberhart, J.H. Thomassin, T. Juteau, J.C. Touray, G. Ehret, CR Acad. Sci. Paris 294 (II) (1982) 989.
[55] J.L. Crovisier, G. Ehret, J.P. Eberhart, T. Juteau, Sci. Géol. Mém. 36 (1983) 197.
[56] J.L. Crovisier, J. Honnorez, J.P. Eberhart, Geochim. Cosmochim. Acta 51 (1987) 2977.
[57] B.C. Bunker, D.R. Tallant, R.J. Kirkpatrick, G.L. Turner, Phys. Chem. Glasses 31 (1990) 30.
[58] A.V. Loshagin, E.P. Sosnin, Glass Phys. Chem. 20 (1994) 250.
[59] W.J. Dell, P.J. Bray, S.Z. Xiao, J. Non-Cryst. Solids 58 (1983) 1.
[60] M.E. Fleet, S. Muthupari, J. Non-Cryst. Solids 255 (1999) 233.
[61] S. Ricol, Thesis, Université Paris VI, 1995.